Reduced north Atlantic deep water coeval with the glacial lake Agassiz freshwater outburst

Helga Flesche Kleiven, Catherine Kissel, Carlo Laj, Ulysses Ninnemann, Thomas Richter, Elsa Cortijo

Reduced North Atlantic Deep Water Coeval with the Glacial Lake Agassiz Freshwater Outburst

Helga (Kikki) Flesche Kleiven,[1,3]* Catherine Kissel,[2] Carlo Laj,[2] Ulysses S. Ninnemann,[1,3] Thomas O. Richter,[4] Elsa Cortijo[2]

An outstanding climate anomaly 8200 years before the present (B.P.) in the North Atlantic is commonly postulated to be the result of weakened overturning circulation triggered by a freshwater outburst. New stable isotopic and sedimentological records from a northwest Atlantic sediment core reveal that the most prominent Holocene anomaly in bottom-water chemistry and flow speed in the deep limb of the Atlantic overturning circulation begins at ~8.38 thousand years B.P., coeval with the catastrophic drainage of Lake Agassiz. The influence of Lower North Atlantic Deep Water was strongly reduced at our site for ~100 years after the outburst, confirming the ocean's sensitivity to freshwater forcing. The similarities between the timing and duration of the pronounced deep circulation changes and regional climate anomalies support a causal link.

An abrupt cooling event ~8200 years before the present (B.P.) [centered between 8.21 and 8.14 thousand years (ky) B.P. (*1*)] is the most extreme climatic anomaly in the Greenland ice core $\delta^{18}O$ records during the otherwise relatively quiescent Holocene period (*2*–*4*). Associated anomalies in various marine and terrestrial proxy records demonstrate that climate change at this time, although most pronounced in Greenland and around the North Atlantic, had a broad and variable expression within the Northern Hemisphere and tropics (*5*, *6*). Identifying the antecedents of such an unusually extreme and widely felt Holocene perturbation is important, particularly for predicting how climate may change, but records that can be used to test the mechanisms hypothesized to have caused the event have been elusive.

Alley *et al.* (*4*) originally postulated that this climate anomaly could have been driven by changes in ocean overturning circulation. If correct, the 8.2 ky B.P. event provides an invaluable case study for understanding both the stability of ocean overturning circulation during warm climate states and the sensitivity of the climate system to any such changes. However, because of the disparate geographic and temporal expression of the climate anomaly, it has been difficult to verify whether the ocean was involved (*6*), let alone delineate its influence. Hence, a prerequisite for any analysis of the nature of climate-ocean coupling across the 8.2 ky B.P. event is an understanding of the changes in ocean circulation at this time.

The occurrence of the outburst flood from proglacial Lake Agassiz on the southwest margin of the retreating Laurentide Ice Sheet into the North Atlantic via the Hudson Strait at 8.47 ± 0.3 ky B.P. (*7*), preceding or potentially coeval with the 8.2 ky B.P. event, supports the idea that ocean circulation may have at least changed at this time, because the freshwater outburst provides a plausible trigger for altering ocean overturning circulation. Using the estimated volume of the outburst flood [e.g., (*8*, *9*)], several model studies show that such a flood is capable of triggering ocean overturning changes that could result in climate anomalies quantitatively similar to those observed in many areas (*10*–*12*). Yet, paleoceanographic observations of deep ocean circulation changes at the time of either the outburst flood or the climate anomaly are equivocal. A number of studies have observed changes in the deep North Atlantic circulation and properties around the 8.2 ky B.P. event (*13*, *14*), but these changes are similar in magnitude to those that have occurred repeatedly during the Holocene. The question remains whether this is because no anomalously large circulation event accompanied the 8.2 ky B.P. climate anomaly or because these sediment records lack the resolution to faithfully reflect such a brief event (*15*).

As a first step in addressing this question, Ellison *et al.* (*16*) demonstrate that it is possible to resolve decadal-century scale bottom-water circulation changes in the early Holocene using suitably expanded sediment records. Using a bottom-water flow-speed proxy to reconstruct changes in Iceland-Scotland Overflow Water, Ellison *et al.* (*16*) show that one of the two major branches of the Nordic Seas overflows was reduced just after the Lake Agassiz freshwater outburst. Although detailed, their deep-water record spans only ~2000 years and thus cannot resolve whether the observed deep-water changes were anomalously large relative to others during the Holocene. In addition, given that only half of the total flux in the Nordic Seas overflows exits through the Eastern branches (*17*, *18*), it is unclear whether the integrated overflows were reduced after the freshwater outburst or whether the western (Denmark Strait) overflow simply increased in compensation, as model results suggest could happen (*19*). Hence, to assess the sensitivity of meridional overturning circulation (MOC) to the Agassiz freshwater out-

[1]Bjerknes Centre for Climate Research, University of Bergen, N-5007 Norway. [2]Laboratoire des Sciences du Climat et de l'Environnement, 91198 Gif-sur-Yvette, France. [3]Department of Earth Science, University of Bergen, N-5007 Norway. [4]Royal Netherlands Institute for Sea Research, 1790 AB Den Burg, Netherlands.

*To whom correspondence should be addressed. E-mail: kikki@uib.no

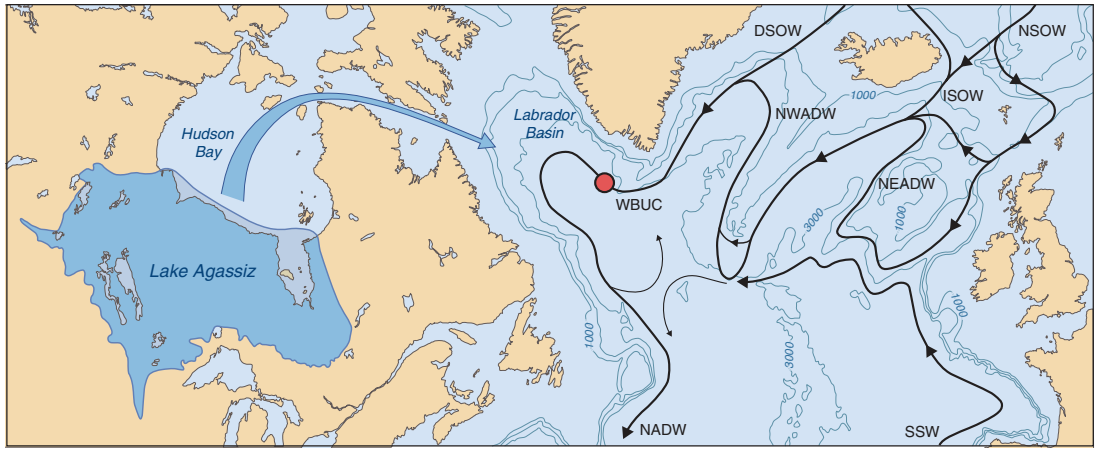

Fig. 1. Map of study area with the location of core MD03-2665 (57°26.56N, 48°36.60W; 3440-m water depth) marked with a red circle. The black arrows indicate the overflows and spreading pathways of deep and intermediate currents, after (*21*, *35*, *36*). The total area covered by Lake Agassiz is shaded, and the general routing of the overflow and outburst through the Hudson bay to the North Atlantic is marked with a blue arrow [modified after (*9*)].

burst, a characterization of the integrated Nordic seas overflows is required.

Here, we present records of deep ocean circulation and chemical properties from Eirik Drift core MD03-2665 (57°26.56N, 48°36.60W; 3440-m water depth) (Fig. 1). This site is sensitively situated and provides the temporal fidelity to detect whether changes in deep-water properties and circulation accompanied the Lake Agassiz outburst. The Eirik Drift accumulates rapidly as a result of the influx of sediments eroded from the Denmark Strait and eastern Greenland margin suspended in Denmark Strait Overflow Water (DSOW) (*20*). DSOW combines with North West Atlantic Deep Water (NWADW) to form the Western Boundary Undercurrent (WBUC) (*21*). The seafloor at site MD03-2665 lies just below the main axis of the sediment-laden WBUC and hence preserves expanded interglacial intervals (*22*). Thus, this location is well situated to monitor changes in the past circulation and properties of newly formed Lower North Atlantic Deep Water (LNADW) along its western boundary flow path. The interval from 0 to 11 ky B.P. is dated by 24 ^{14}C accelerator mass spectrometry (AMS) dates (table S1 and figs. S3 and S4). The average sedimentation rates (90 cm/ky from 10.7 to 8.5 ky B.P., >200 cm/ky from 8.5 to 8.2 ky B.P., and 40 cm/ky thereafter) are suitable for resolving even brief circulation anomalies such as those simulated in response to the Lake Agassiz outburst (*23*).

Eirik Drift proxy records. To assess the timing, amplitude, and nature of deep-water changes during the past 10 ky, we have generated a suite of high-resolution sedimentary, geochemical, and magnetic proxy data (Fig. 2 and Supporting Online Material). The most striking feature in all of our records is the large deviation beginning at 3.45-m core depth. Our epibenthic carbon isotope record

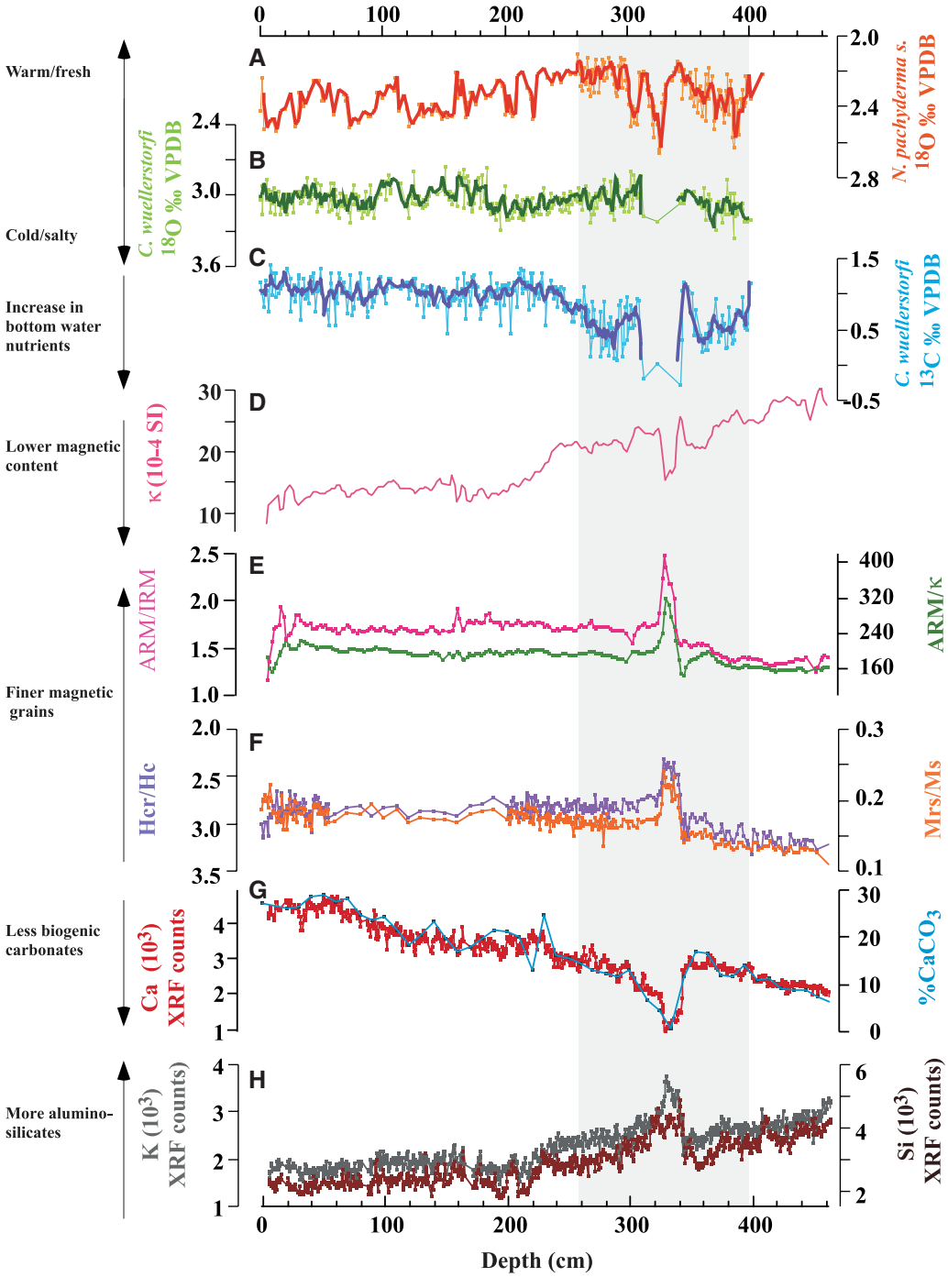

Fig. 2. Proxy records along the Holocene section of core MD03-2665 plotted versus depth. (**A**) *Neogloboquadrina pachyderma* sinistral coiling $\delta^{18}O$‰ VPDB plotted with a 5-point running mean. (**B**) *Cibicidoides wuellerstorfi* $\delta^{18}O$‰ VPDB plotted with a 5-point running mean. (**C**) *Cibicidoides wuellerstorfi* $\delta^{13}C$‰ VPDB plotted with a 5-point running mean. (**D**) Low-field magnetic susceptibility. (**E**) Anhysteretic remanent magnetization/isothermal remanent magnetization (ARM/IRM) and ARM/κ ratios as proxies for magnetic grain size. (**F**) Hcr/Hc and Mrs/Ms hysteresis ratio also illustrating changes in magnetic domain states related to magnetic grain sizes. (**G**) Ca element measured every 5 mm by XRF scanning superimposed to $CaCO_3$ percentages measured at lower resolution. (**H**) Potassium (K) and silicon (Si) major elements. The shaded area highlights the study interval shown in Figs. 3 and 4 (i.e., 7300 to 9300 calendar years B.P.).

(Fig. 2C) implies a pronounced shift in the chemistry of bottom waters bathing the site: $\delta^{13}C$ decreases sharply from average Holocene values of about 1 per mil (‰) [Vienna Pee Dee belemnite (VPDB)] to below 0‰ over a few centimeters, followed by a similarly sharp recovery at ~3.15-m core depth.

Concurrently, the magnetic properties and sedimentary composition of the core also change dramatically at 3.45 m (Fig. 2, D to H). The magnetic properties indicate that magnetite is the main magnetic carrier (*S*-ratio close to unity and Curie temperature at about 570 to 580°C; see supporting online material) and that its average grain size fines abruptly in this interval, in contrast to an otherwise uniform magnetic grain size throughout the past 10 ky. In addition, the concentration in magnetic particles is reduced twofold during the episode. The two main transport vectors for magnetic particles in the North Atlantic are bottom currents carrying large amounts of magnetite-rich sediments originating from the Nordic basaltic provinces and iceberg discharges. The latter are characterized by episodic supplies of poorly sorted magnetic grains, resulting in a clear coarsening of the magnetic fraction (*24*). In addition, the amount of magnetic minerals associated with iceberg discharges is much smaller than the magnetic load transported by the main deep currents. This is true even along the main path of icebergs, where discharges are at a maximum, and also during periods when the magnetic fraction undergoes a twofold decrease, along the path of the bottom current (*25*). Therefore, at this site changes in the magnetic contents most likely illustrate changes in the passive transport of magnetic particles, i.e., changes in the strength of the DWBUC at the core depth (*26*). Thus, the sharp reduction in the number and size of magnetic grains suggests that there was a rapid decrease in bottom-current activity transporting magnetic grains to this site.

Concomitantly, major element analyses done with x-ray fluorescence (XRF) scanning show a marked drop in the Ca contents, while the aluminosilicate–derived elements K and Si increase by about 60%. $CaCO_3$ percentages abruptly decrease from 17% to 0.6%, subsequently recovering to values of about 20% after the event. These changes coincide with an apparent abrupt increase in sedimentation rates as inferred from the AMS ^{14}C chronology (see Supporting Online Material). The pronounced change in bulk sediment chemical composition indicates dilution of biogenic carbonate by fine-grained terrigenous material. The coincidence in timing of this sedimentary event with the Lake Agassiz flood points toward the outburst as the source of fine material, although the lack of detrital carbonate (found in very proximal outburst sediments) may suggest that the sedimentary changes originate from other source regions or WBUC fluctuations (*27*). In all proxies, the onset of the event is very abrupt, occurring within a few centimeters, whereas the return to average Holocene values is slightly more gradual, at least in the proxies that were measured continuously. Thus, all of our proxies show a synchronous geochemical and sedimentological anomaly that is the most prominent one within the Holocene.

Deep-water changes. What could have driven such an anomalously large and abrupt change coevally in our proxies of deep-water chemistry and flow, as well as sedimentary composition? The inferred increase in bottom-water nutrients, decrease in sediment biogenic content, and weakening bottom-current activity with decrease in magnetic grain size and concentration are all consistent with a sudden and pronounced decrease of LNADW influence at the site. The lower benthic $\delta^{13}C$ values generally observed before 7.5 ky B.P. are consistent with previous suggestions that not all components of NADW were at modern strength in the early Holocene (*27*, *28*). However, it is notable that just before the extreme event, benthic foraminiferal $\delta^{13}C$ values rise to just over 1‰ versus VPDB—similar to late Holocene North Atlantic core top values (*29*)—suggesting that the site was bathed by a low-nutrient water mass isotopically similar to modern LNADW. The subsequent decrease in foraminiferal $\delta^{13}C$ of over 1‰ in just a few centimeters suggests that during the anomaly low-nutrient LNADW was replaced by a high-nutrient deep-water mass.

Because this ventilation change was accomplished very rapidly, over a few decades or less in our age model, it was most likely related to changing deep-circulation dynamics and shifting of water-mass boundaries relative to our site rather than solely caused by a gradual accumulation of nutrients related to a slowdown in ventilation. The most likely explanation is that the boundary between LNADW (high $\delta^{13}C$) and southern source deep water (low $\delta^{13}C$) shoaled across our core site. The fact that our benthic $\delta^{13}C$ values drop to levels equivalent to those found in Southern Ocean deep waters during the early Holocene (*30*) strongly supports this scenario. The decrease in bottom-current activity indicated by the decrease in magnetic grain size and concentration in our core is also consistent with a shoaled or decreased DWBUC and may be the equivalent of the oceanographic event recorded in other sites below the DWBUC previously dated at ~8.8 ky B.P. (*27*).

The reduced influence of low-nutrient LNADW at our site from ~8.38 to 8.27 ky B.P. suggests that a shoaling and perhaps a reduction in the MOC occurred at this time. Because our site lies near the base of the bounding topography guiding the DWBUC on its westward path, the combined Nordic Seas overflows should influence our location provided they are dense enough. Our results show that for ~100 years none of the Nordic Seas overflows produced low-nutrient deep water dense enough to mix down to 3440 m. Model studies (*31*) suggest that on decadal time scales the MOC transport is highly sensitive and linearly related to

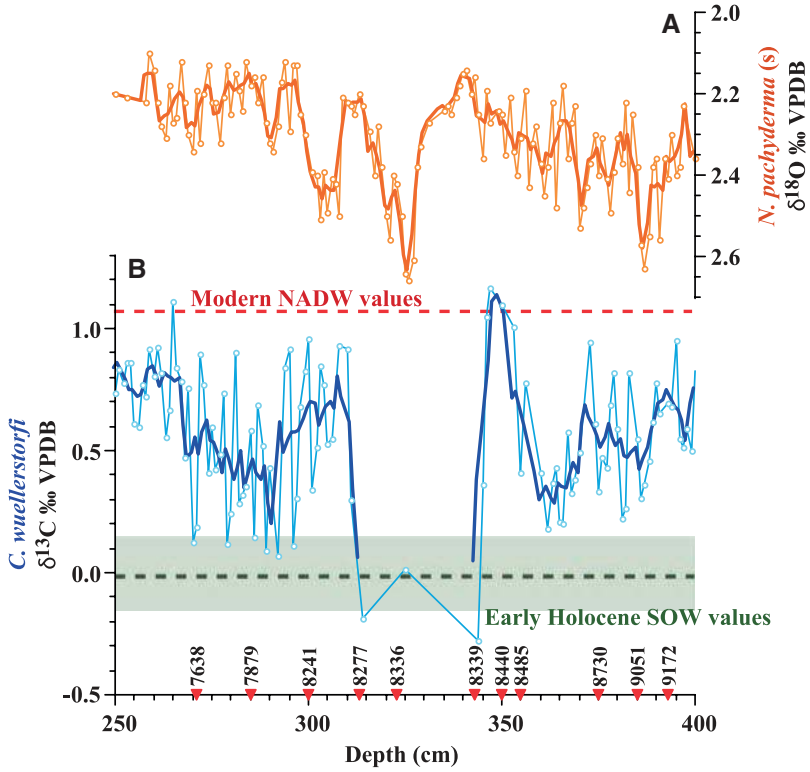

Fig. 3. (**A**) *Neogloboquadrina pachyderma* sinistral coiling $\delta^{18}O$‰ VPDB plotted with a 5-point running mean and (**B**) *Cibicidoides wuellerstorfi* $\delta^{13}C$‰ VPDB plotted with a 5-point running mean. Both records are plotted versus depth in the core. Typical Holocene NADW $\delta^{13}C$ values are indicated by the red dashed line (*29*); Holocene SOW $\delta^{13}C$ mean values and 1σ variance (taken from core TN057-15) are indicated by the green dashed line and the shaded bar, respectively (*30*). Position and calibrated ages of the AMS ^{14}C dated levels in this interval are indicated along the depth axes in red triangles.

the density of DSOW, the most influential water mass at our core site today. Thus, the overall vigor of MOC is likely to have decreased in tandem with the drop in overflow density, provided that such sensitivity studies apply to longer time scales. A centennial reduction in Nordic Seas overflows (the deep limb of MOC) is consistent with the observation that the northward flux of warm Atlantic water in the Nordic Seas (the upper limb of the MOC) was also reduced for ~100 years around the 8.2 ky B.P. event (*32*).

The fact that the only anomalously large disruption in the deep southward flowing branch of the MOC occurs coevally with the largest known outburst of freshwater to the North Atlantic, the Lake Agassiz outburst, supports the hypothesis that MOC is sensitive to freshwater forcing. Indeed, our inference that the density, and perhaps the flux, of the southward flowing branch of the MOC were decreased matches model predictions for the nature and timing of the deep-water response to the Lake Agassiz outburst (*23*, *33*). The rate at which the deep-water changes are accomplished in our core demonstrates that these shifts in deep-ocean circulation can occur in perhaps as little as a few decades, even in warm climate states, just as models predict [e.g., (*23*)].

Surface ocean response. Having defined the timing and duration of the deep circulation anomaly associated with the outburst, it is possible to consider more explicitly the impact of these circulation changes on climate. Our site is located near the bull's-eye of the cooling related to MOC weakening in many model experiments (*10*, *23*). If taken to solely reflect temperature, planktonic foraminiferal $\delta^{18}O$ at our site indicate a sharp near-surface cooling of ~1.5°C, but only ~15 cm after the initiation of the deep-circulation event (Fig. 3). This suggests either that there was no local cooling accompanying the initial perturbation in ocean circulation or that the influence of any cooling was offset by changes in the $\delta^{18}O$ of water at this location. Model studies suggest that the freshwater from the Agassiz outburst could indeed dampen or offset the effects of cooling on planktonic $\delta^{18}O$ (*10*), and paired planktonic Mg/Ca and $\delta^{18}O$ records suggest that this damping did occur south of Iceland during the 8.2 ky B.P. event (*34*). Another possibility is that the delay was real. Taken at face value, this offset might suggest that changes in ocean circulation are more of a prerequisite for, rather than a direct driver of, the 8.2 ky B.P. cooling event. Yet, as sedimentation rates increased dramatically at the onset of the deep-water anomaly, this depth offset may represent a time delay of only a couple of decades—and much less if the increased sedimentation rate was due to a pulsed input of sediments.

Despite the apparent offset in duration between the climate and deep ventilation changes co-registered in our core, two points strongly support a connection: (i) at our site, the largest surface ocean cooling (planktonic $\delta^{18}O$ increase) during the Holocene occurs during the period when NADW influence is weakest, and (ii) the magnitude of the cooling event and the nature of the deep circulation change are both similar to those modeled in response to a freshwater-induced slowdown of MOC. Furthermore, it is likely that the surface cooling associated with the deep-water changes in our core is the local equivalent of the strong but brief 8.2 ky B.P. cooling observed in circum-Atlantic records because it is coeval (within the dating uncertainties) with the anomalously large cooling observed in marine and Greenland ice core temperature proxies (Fig. 4). Seen in this way, our proxy records provide a means of delineating which parts of the compound climate signal around 8.2 ky B.P. could be related to ocean circulation changes—the weaker multicentennial cooling versus the much stronger cooling event superimposed on this, which lasted <100 years. Although Ellison *et al.* (*16*) find that the eastern branch of the Nordic Seas overflow was reduced for ~400 years after the flood outburst, our findings suggest that the perturbation in the integrated Nordic Seas overflows was much shorter (~100 years) and much more closely matches the timing and duration of the southerly advance of polar waters inferred by Ellison *et al.* (*16*) (Fig. 4). This suggests that only the brief and anomalously strong portion of the 8.2 ky B.P. cooling seen in Greenland and North Atlantic records was associated with a reduction of southward-flowing NADW (Fig. 4).

Our co-registered climate and deep-water records show other periods in which climate and circulation changed in concert. For example the second largest Holocene cooling (planktonic $\delta^{18}O$ increase) in our record, centered at ~9.1 ky B.P., is also associated with a decrease in LNADW (benthic $\delta^{13}C$) at our site (Fig. 4). However, it is clear that not

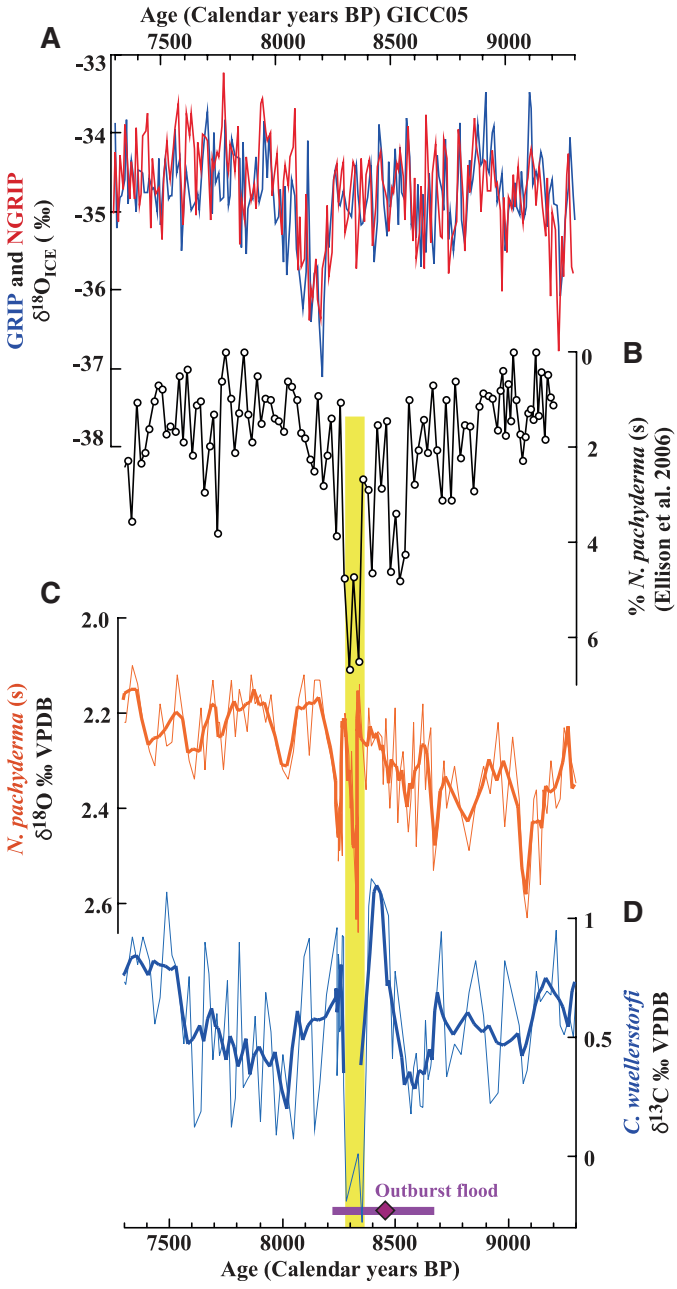

Fig. 4. Paleoceanographic records along core MD03-2665 compared with *Neogloboquadrina pachyderma* (sinistral coiling) percentage counts from core MD99-2251 and NGRIP and GRIP ice core data over the interval 7300 to 9300 calendar years B.P. (**A**) NGRIP and GRIP $\delta^{18}O_{ice}$‰ after (*37*) plotted on the ice core chronology of (*38*, *39*). (**B**) Percentage *Neogloboquadrina pachyderma* sinistral coiling after (*16*). (**C**) *Neogloboquadrina pachyderma* sinistral coiling $\delta^{18}O$‰ VPDB plotted with a 5-point running mean. (**D**) *Cibicidoides wuellerstorfi* $\delta^{13}C$‰ VPDB plotted with a 5-point running mean. The yellow vertical bar highlights the interval where LNADW influence is inferred to be absent at our site. Also shown is the age for the Lake Agassiz drainage event: 8470 years B.P. (*7*) (purple diamond), with its 1 SD uncertainties (8160 to 8740 years B.P.) denoted by a purple line. The age model used for (C) and (D) is described in the Supporting Online Material.

every change in surface climate at our site has an accompanying change in deep circulation (and vice versa)—emphasizing even more strongly the uniqueness of the coeval extremes in climate and deep circulation that follow the Lake Agassiz flood outburst.

Wider climatic implications. Despite the complex nature of the climate record, the fact that large-scale changes in deep-ocean circulation are accomplished just as quickly in the natural world as is predicted in computer simulations [e.g., (*12*)] confirms that they were sufficiently rapid to be a plausible mechanism for driving the similarly abrupt changes seen in paleoclimate records. This observation helps to define the minimum time scale for altering ocean circulation and demonstrates that it is rapid enough to be relevant for human societies. The fact that these past ocean circulation changes are associated with the largest climate variations in the past underscores the importance of understanding the minimum freshwater forcing capable of affecting such large circulation changes—particularly given the concerns about the impact of future warming on the Greenland ice sheet.

References and Notes

1. E. R. Thomas *et al*., *Quat. Sci. Rev.* **26**, 70 (2007).
2. S. J. Johnsen *et al*., *Nature* **359**, 203 (1992).
3. W. Dansgaard *et al*., *Nature* **364**, 218 (1993).
4. R. B. Alley *et al*., *Geology* **25**, 483 (1997).
5. R. B. Alley, A. M. Ágústdóttir, *Quat. Sci. Rev.* **24**, 1123 (2005).
6. E. J. Rohling, H. Pälike, *Nature* **434**, 975 (2005).
7. D. C. Barber *et al*., *Nature* **400**, 344 (1999).
8. D. W. Leverington, J. D. Mann, J. T. Teller, *Quat. Res.* **57**, 244 (2002).
9. J. T. Teller, D. W. Leverington, J. D. Mann, *Quat. Sci. Rev.* **21**, 879 (2002).
10. A. N. LeGrande *et al*., *Proc. Natl. Acad. Sci. U.S.A.* **103**, 837 (2006).
11. E. Bauer, A. Ganopolski, *Paleoceanography* **19**, PA3014 (2004).
12. A. P. Wiersma, H. Renssen, *Quat. Sci. Rev.* **25**, 63 (2006).
13. I. R. Hall, G. G. Bianchi, J. R. Evans, *Quat. Sci. Rev.* **23**, 1529 (2004).
14. D. W. Oppo, J. McManus, J. D. Cullen, *Nature* **422**, 277 (2003).
15. L. D. Keigwin, J. P. Sachs, Y. Rosenthal, E. A. Boyle, *Paleoceanography* **20**, PA2003 (2005).
16. C. R. W. Ellison, M. R. Chapman, I. R. Hall, *Science* **312**, 1929 (2006).
17. B. Hansen, S. Østerhus, *Prog. Oceanogr.* **45**, 109 (2000).
18. B. Hansen, W. R. Turrell, S. Østerhus, *Nature* **411**, 927 (2001).
19. A. Biastoch, R. H. Kase, D. B. Stammer, *J. Phys. Oceanogr.* **33**, 2307 (2003).
20. C. N. Wold, *Paleoceanography* **9**, 917 (1994).
21. M. S. McCartney, *Prog. Oceanogr.* **29**, 283 (1992).
22. C. Hillaire-Marcel, A. de Vernal, G. Bilodeau, G. Wu, *Can. J. Earth Sci.* **31**, 63 (1994).
23. A. P. Wiersma, H. Renssen, H. Gosse, T. Fichefet, *Clim. Dyn.* **27**, 831 (2006).
24. C. Kissel, *C.R. Acad. Sci. Paris* **337**, 908 (2005).
25. J. S. Stoner, J. E. T. Channell, C. Hillaire-Marcel, *Paleoceanography* **11**, 309 (1996).
26. C. Kissel *et al*., *Earth Planet. Sci. Lett.* **171**, 489 (1999).
27. C. Hillaire-Marcel, A. de Vernal, D. J. W. Piper, *Geophys. Res. Lett.* **34**, L15601 (2007).
28. C. Hillaire-Marcel, A. de Vernal, G. Bilodeau, A. J. Weaver, *Nature* **410**, 1073 (2001).
29. W. B. Curry, D. W. Oppo, *Paleoceanography* **20**, PA1017 (2005).
30. U. S. Ninnemann, C. D. Charles, *Earth Planet. Sci. Lett.* **201**, 383 (2002).
31. M. Latif *et al*., *J. Clim.* **19**, 4631 (2006).
32. D. Klitgaard-Kristensen, H. P. Sejrup, H. Haflidason, S. Johnsen, M. Spurk, *J. Quat. Sci.* **13**, 165 (1998).
33. H. Renssen, H. Goosse, T. Fichefet, J.-M. Campin, *Geophys. Res. Lett.* **28**, 1567 (2001).
34. R. E. Came, D. W. Oppo, J. F. McManus, *Geology* **35**, 315 (2007).
35. W. J. Schmitz, M. S. McCartney, *Reviews of Geophysics* **31**, 29 (1993).
36. R. R. Dickson, J. Brown, *J. Geophys. Res.* **99**, 12319 (1994).
37. S. O. Rasmussen, B. M. Vinther, H. B. Clausen, K. K. Andersen, *Quat. Sci. Rev.* **26**, 1907 (2007).
38. S. O. Rasmussen *et al*., *J. Geophys. Res.* **111**, D06102 (2006).
39. B. M. Vinther *et al*., *J. Geophys. Res.* **111**, D13102 (2006).

40. We thank the Centre for Ice and Climate (especially B. Vinther, S. Johnsen, and S. Rasmussen) at the Niels Bohr Institute at University of Copenhagen, for supplying the unpublished GRIP and NGRIP data. We are also grateful for technical assistance from D.-I. Blindheim, E. Bjørseth, E. V. Galaasen, O. Hansen, and I. V. Johansen from Bjerknes Centre for Climate Research (BCCR)/University of Bergen (UoB) and C. Wandres and F. Dewilde from Laboratoire des Sciences du Climat et de l'Environnement (LSCE), Commisariat à l'Energie Atomique (CEA), Centre National de la Recherche Scientifique (CNRS), Université Versailles-Saint-Quentin (UVSQ). This work was supported by the BCCR, the UoB, and the Norwegian Research Council, and at LSCE by the CEA and CNRS through the Institut des Sciences de l'Univers, Programme National d'Etude du Climat (INSU-PNEDC-Impair) project. Additional funding was provided by the PACLIVA EU EVK2-2002-00143 and the Agence National de la Recherche, Integration des Contraintes Paléoclimatiques: Réduire les Incertitudes sur l'Evolution du Climat des Périodes Chaudes (ANR-PICC) projects. The GIFA ^{14}C dates were obtained by AMS Artemis from LMC14, National Service of INSU. We are grateful to M. Paterne (LSCE) for her help with the GIFA ^{14}C data. The ship and scientific technology for the P.I.C.A.S.S.O. cruise were provided by the Institut Polaire Paul Emile Victor (IPEV) within the framework of the International Marine Global Changes (IMAGES) program. H.F.K. and U.S.N. analyzed the planktonic and benthic stable isotope data in this study and prepared samples for the KIA AMS ^{14}C dates. E.C. was responsible for the paleoceanographic team in LSCE. C.K. and C.L. are responsible for the magnetic and $CaCO_3$ analyses reported here and C.L. was chief scientist on P.I.C.A.S.S.O. T.O.R. is responsible for the x-ray fluorescence scans.

Supporting Online Material for

Reduced North Atlantic Deep Water Coeval with the Glacial Lake Agassiz Fresh Water Outburst

Helga (Kikki) Flesche Kleiven,* Catherine Kissel, Carlo Laj,
Ulysses S. Ninnemann, Thomas O. Richter, Elsa Cortijo

*To whom correspondence should be addressed. E-mail: kikki@uib.no

This PDF file includes:

Supporting Online Material

Materials and methods

Stable Isotopes.

Core MD03-2665 was sampled continuously at 1 cm interval. Each sample was placed in distilled water and left for 12 hr on a shaking table to disaggregate. The samples were then wet sieved into two fractions: >63-µm and >150-µm. Following this, the coarse fraction was dried and transferred to sample glasses. The planktonic foraminiferal isotopic analyses were performed on 8 to 10 individual tests of *Neogloboquadrina pachyderma* sinistral coiling, selected from the 150-250-µm size fraction, whereas the benthic foraminiferal isotopic analyses were performed on 1-2 specimens of the epifaunal benthic foraminifera *Cibicidoides wuellerstorfi,* picked from the >250-µm fraction. Due to the low abundance of *Cibicidoides wuellerstorfi,* not all samples could be run as duplicates or triplicates. Replicate analyses were done if sufficient foraminifera were found. The final *Neogloboquadrina pachyderma* sinistral coiling oxygen isotope record corresponds to average values of 2 replicates every 4 cm (0-340 cm), and high-resolution measurements (1 every cm) from 253-400 cm. Replica values for *Cibicidoides wuellerstorfi* δ^{13}C‰ VPDB with an averaged mean are plotted in figure S1 below. Replica values for *Neogloboquadrina pachyderma* sinistral coiling δ^{18}O‰ VPDB with an averaged mean are plotted in figure S2 below.

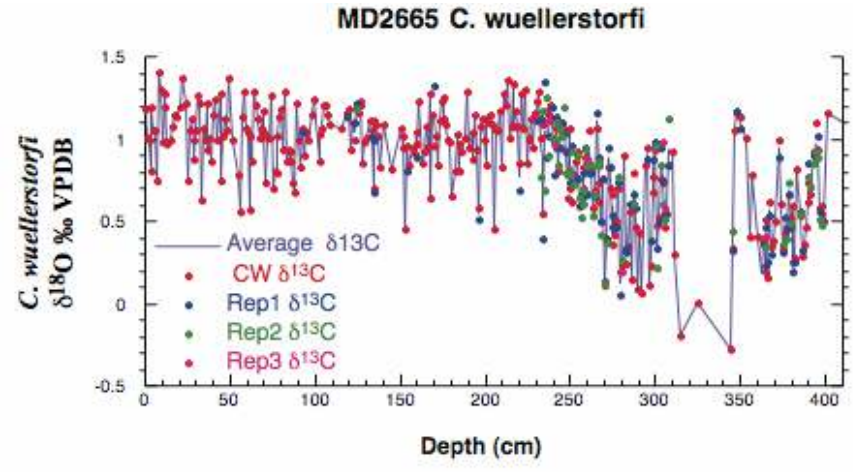

Figure S1 Replica values for *Cibicidoides wuellerstorfi* δ^{13}C‰ VPDB (red, blue, green and pink dots) with an averaged mean (purple line) from core MD03-2665 plotted versus depth.

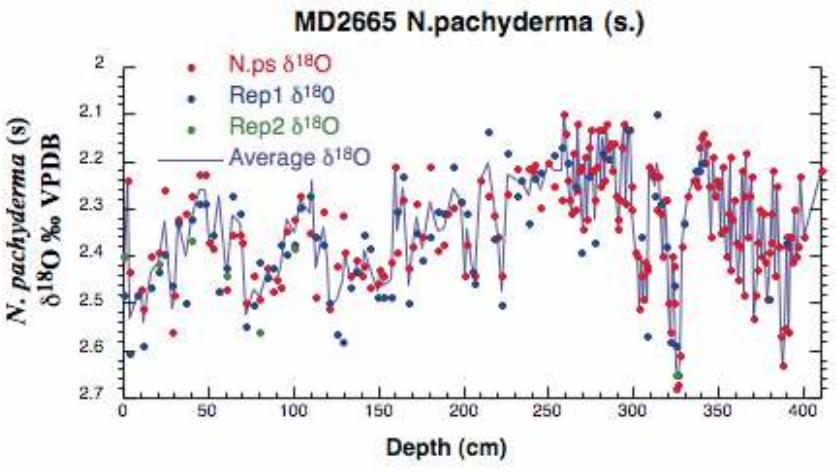

Figure S2 Replica values for *Neogloboquadrina pachyderma* sinistral coiling $\delta^{18}O$‰ VPDB (red, blue and green) with an averaged mean (purple line) from core MD03-2665 plotted versus depth.

Before analyses the foraminiferal shells were ultrasonically rinsed for 20 seconds in methanol to remove fine-grained particles. The methanol was removed using a syringe and the samples dried in a drying cabinet. The foraminifer shells were then loaded into individual reaction glasses, and each sample was reacted with three drops of H_3PO_4 using an automated Kiel device preparation line. Isotope ratios were measured on a Finnigan MAT 251 mass spectrometer (*Neogloboquadrina pachyderma* sinistral coiling) and on a Finnigan MAT 253 mass spectrometer (*Neogloboquadrina pachyderma* sinistral coiling and *Cibicidoides wuellerstorfi*) at the stable isotope laboratory at BCCR/Department of Earth Sciences, University of Bergen. The working standard measured parallel with the samples is Carrera Marble (CM03). The isotopic values are calibrated to VPDB using NSB-19. Long-term analytical precision (1σ) of the standards over a time interval of several months is 0.1‰ and 0.04‰ for $\delta^{18}O$ and $\delta^{13}C$ respectively for samples weighing 7-50µg on the MAT 253 system and <0.08‰ and 0.04‰ for $\delta^{18}O$ and $\delta^{13}C$ respectively for the MAT 251 system.

Magnetic properties.

For the analyses of the magnetic properties, core MD03-2665 was sub-sampled using u-channels, which were measured in the shielded room of the magnetic laboratory of the LSCE. The u-channels were using a 2G-Enterprises Model 755 cryogenic magnetometer at 2 cm intervals. The spatial resolution of the pick-up coils is ~ 4.5 cm. Edge effects were removed from the final data. Anhysterestic Remanent Magnetization (ARM) was produced in line along the Z-axis of the u-channels with 0.1 T peak AF in a 50 m T DC field. ARM was demagnetized with 10 AF steps from 10 to 80mT. Isothermal Remanent Magnetization was induced stepwise using an in-line pulsed solenoid with fields of 0.05, 0.1, 0.2, 0.3, 0.5 and 1T. A reverse IRM was then imparted in a field of 0.3 T to calculate the S-ratio. The 1T IRM was AF demagnetized using the same steps as for ARM. Low-field magnetic susceptibility was measured on a separate set-up using a Bartington MS2C

45 mm diameter coil, which has the same spatial resolution as the cryogenic magnetometer.
An alternating gradient magnetometer (AGM 2900) was used for hysteresis analysis of small amounts of sediment taken at 10 cm intervals through the Holocene. The sampling interval was reduced to 1 between 0 and 55 cm and between 200 and 350 cm and to 20 cm between 352 and 450 cm.

X-ray fluorescence (XRF) logging.
Semi-quantitative major and minor element determinations were carried out at Royal NIOZ with the AVAATECH XRF core scanner (*S1*) . These analyses were performed on the surface of the u-channels with a step size of 5 mm, operating voltage of 10kV and count time of 30 seconds per sample. Results are presented as total XRF counts which correspond to the peak areas for respective elements.

Calcium carbonate content.
The carbonate content (in %) have been measured using the manocalcimeter of the IDES Department at the University of Orsay (France). 100 mg samples taken at 10 cm interval in the core have been mixed with HCl (6N) in a closed vial (22.4 cm^3). The manocalcimeter has systematically been standardized so that 1 bar corresponds to 100 mg of $CaCO_3$.

Chronology
We obtained 23 accelerator mass spectrometry (AMS) ^{14}C ages on mixed planktonic foraminifera (Table S1), including 6 dates across the critical time interval from 8.2-8.5 ka calendar. Radiocarbon ages have been converted into calendar ages with the CALIB (rev 5) software (*S2*) and the MARINE04 calibration dataset (*S3*). Most dates were calibrated with a constant surface reservoir age of 400 years. However, for two dates corresponding to pronounced planktonic foraminiferal $\delta^{18}O$ maxima, we applied an additional reservoir age correction (ΔR = 128±23a, average deviation for the East Greenland Current, see http://radiocarbon.pa.qub.ac.uk/marine/). Estimated mean sedimentation rates are ~90cm/ka for the early Holocene (10.7-8.5ka), ~225cm/ka from 8.5-8.2ka, and ~40cm/ka thereafter (Figure S3 and S4 below). Taking calendar ages at face value, very high sedimentation rates occur coevally with the onset of changes in our proxy records, consistent with our interpretation of the sedimentological proxy anomalies as an instantaneous event (see text).

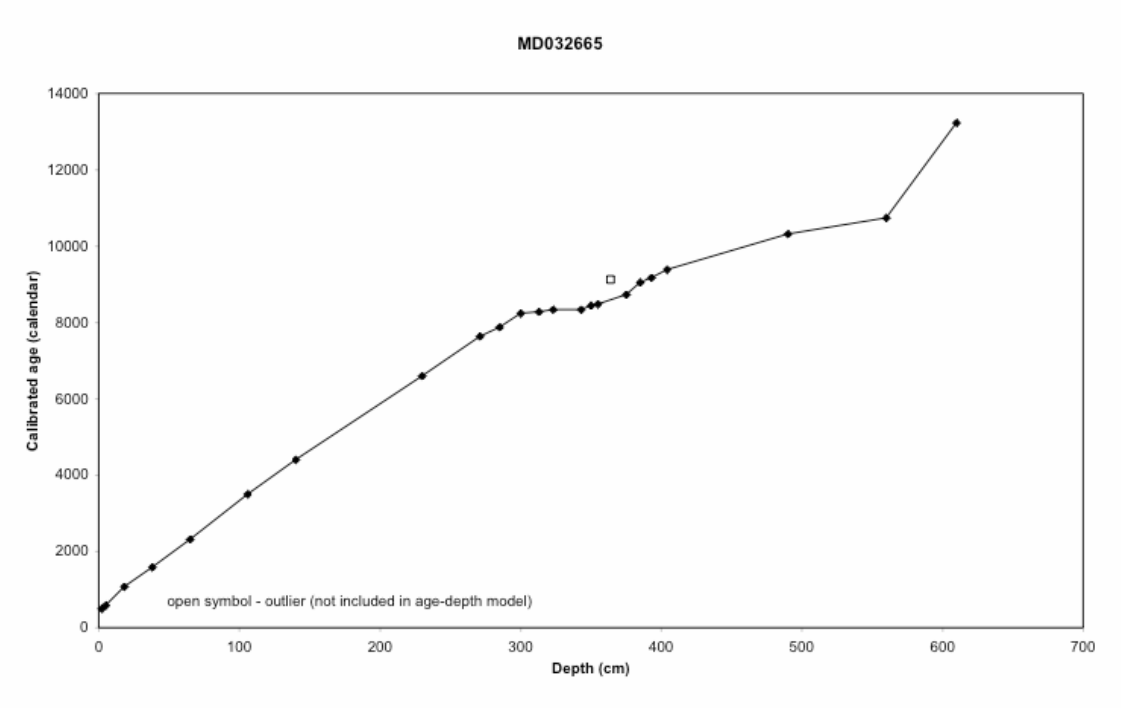

Figure S3. Age-depth relationship of core MD03-2665; 0-700 cm

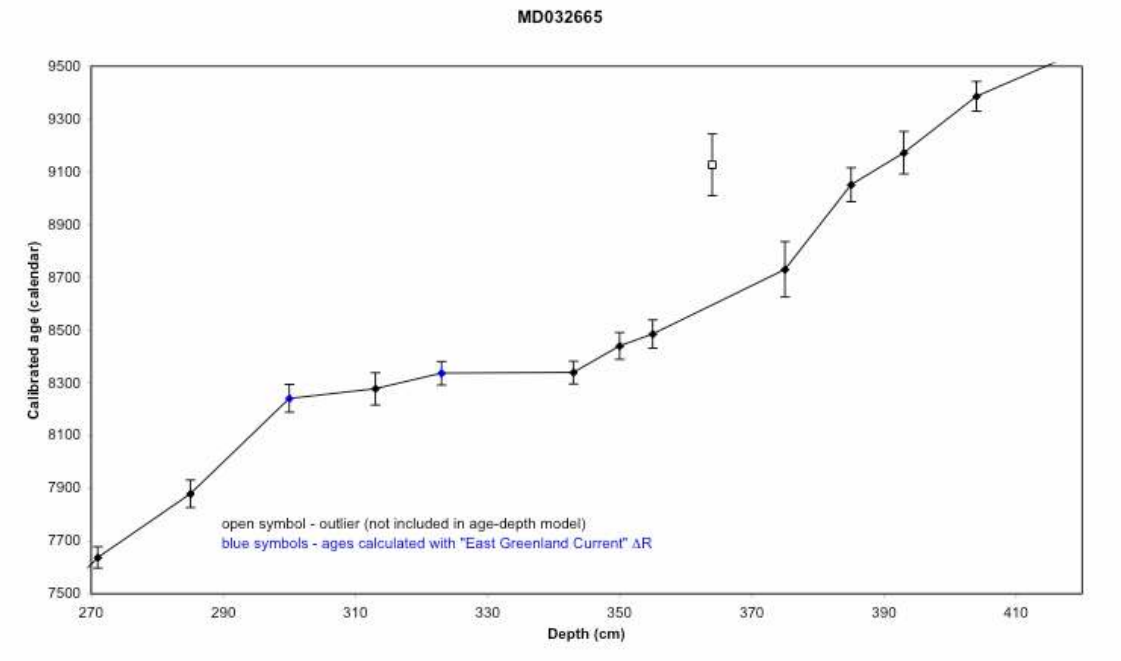

Figure S4. Age-depth relationship of core MD03-2665 with focus on the high-resolution interval from 270-420 cm

Table S1 Radiocarbon ages from core MD03-2665 determined by accelerator mass spectrometry

Depth (cm)	Lab code [a]	Species [b]	Uncorrected ^{14}C age (yr) ± 1σ error	Calendar age BP [c] (median probability)	1σ age range	Remarks
2	KIA	Gbull	890 ± 30	504	482-525	
5	KIA	NPD	995 ± 25	582	549-613	
18	KIA	Gbull	1525 ± 35	1080	1034-1140	
38	KIA	mixed Gbull + NPS	2020 ± 30	1585	1529-1624	
65	KIA	Gbull	2635 ± 30	2320	2288-2348	
106	KIA	Gbull	3605 ± 45	3501	3438-3559	
140	KIA	Gbull	4280 ± 30	4400	4343-4447	
230	KIA	Gbull	6160 ± 30	6597	6550-6644	
271	KIA	mixed Gbull + NPS	7175 ± 30	7638	7592-7673	
285	KIA	mixed Gbull + NPS	7415 ± 50	7879	7829-7933	
300	KIA	NPD	7895 ± 40	8241	8186-8291	ΔR of 128±23a applied (see table caption)
300	*KIA*	*NPD*	*7895 ± 40*	*8361*	*8328-8392*	
313	KIA	mixed Gbull + NPS	7810 ± 35	8277	8214-8338	
323	KIA	mixed Gbull + NPS	7995 ± 40	8336	8294-8384	ΔR of 128±23a applied (see table caption)
323	*KIA*	*mixed Gbull + NPS*	*7995 ± 40*	*8453*	*8401-8499*	
343	KIA	mixed Gbull + NPS	7870 ± 55	8339	8298-8384	
343	KIA	mixed Gbull + NPS	7795 ± 45	8265	8212-8317	duplicate analysis (not used)
350	KIA	mixed Gbull + NPS	7980 ±45	8440	8384-8487	
355	KIA	mixed Gbull + NPS	8030 ±45	8485	8426-8535	
364	GifA	mixed Gbull + NPS	8500 ± 90	9135	9009-9242	outlier (not used)
375	KIA	mixed Gbull + NPS	8215 ± 45	8730	8623-8835	
385	KIA	mixed Gbull + NPS	8435 ± 50	9051	8981-9111	
393	KIA	Gbull	8535 ± 50	9172	9092-9254	
404	KIA	mixed Gbull + NPS	8705 ± 45	9386	9340-9442	
490	GifA	mixed Gbull + NPS	9460 ± 70	10318	10225-10392	
560	GifA	Gbull	9850 ± 60	10744	10601-10879	
610	GifA	NPS	11770 ± 70	13235	13175-13296	

[a] KIA – Leibniz Labor für Altersbestimmung und Isotopenforschung, Kiel, Germany; GifA - Laboratoire des Sciences du Climat et de l'Environnement, sur-Yvette, France [b] Gbull – *G. bulloides*; NPD – *N. pachyderma*(d); NPS – *N. pachyderma*(s)

[c] ^{14}C ages were converted into calendar ages with the CALIB vs.5 software and the MARINE04 calibration dataset. We applied a standard 400a reservoir age correction in most cases, and an additional ΔR for two dates to account for enhanced influence of the East Greenland surface current (inferred from pronounced planktonic foraminiferal δ^{18}O maxima) *Ages in blue are for the standard 400a reservoir effect causing age reversals*

References and notes

S1. T. O. Richter *et al.*, in *New techniques in Sediment Core Analyses* G. Rothwell, Ed. (Geol. Soc. London Spec. Publ., 2006), vol. 267, pp. 39-50.

S2. M. Stuvier, P. J. Reimer, *Radiocarbon* **35**, 215 (1993).

S3. K. A. Hughen *et al.*, *Radiocarbon* **46**, 1059 (2004).